Since January 2020 Elsevier has created a COVID-19 resource centre with free information in English and Mandarin on the novel coronavirus COVID-19. The COVID-19 resource centre is hosted on Elsevier Connect, the company's public news and information website.

Talanta 214 (2020) 120865

Contents lists available at ScienceDirect

Talanta

journal homepage: www.elsevier.com/locate/talanta

EuNPs-mAb fluorescent probe based immunochromatographic strip for rapid and sensitive detection of porcine epidemic diarrhea virus

Fei Xu[a,1], Zhiyuan Jin[a,1], Siyi Zou[a,1], Chaoqun Chen[a], Qifang Song[a], Shengchao Deng[a], Wei Xiao[a], Xiaoli Zhang[a,***], Aiqing Jia[b,**], Yong Tang[a,c,*]

[a] Department of Bioengineering, Guangdong Province Engineering Research Center of Antibody Drug and Immunoassay, Jinan University, Guangzhou, 510632, PR China
[b] Guangdong Haid Institute of Animal Husbandry & Veterinary, PR China
[c] Institute of Food Safety and Nutrition, Jinan University, Guangzhou, 510632, PR China

ARTICLE INFO

Keywords:
Porcine epidemic diarrhea virus
Europium nanoparticle
Immunoassay
Swine stool analysis
Southern China

ABSTRACT

Porcine epidemic diarrhea (PED), induced by porcine epidemic diarrhea virus (PEDV) causes acute diarrhea, vomiting, dehydration and high mortality in neonatal piglets, resulting in significant economic losses in the pig industries. In this study, an immunochromatographic assay (ICA) based on a EuNPs-mAb fluorescent probe was developed and optimized for rapid detection of PEDV. The limit of detection (LOD) of the ICA was 0.218 μg/mL (2.725×10^3 $TCID_{50}$/mL) and its linear detection range was 0.03125–8 μg/mL (3.91×10^{-2}-10^5 $TCID_{50}$/mL). The ICA was also validated for the detection of PEDV in swine stool samples. 60 swine stool samples from southern China were analyzed by the ICA and RT-PCR, and the results showed that the coincidence rate of the ICA to RT-PCR was 86.67%, which was significantly higher than that of AuNPs based ICA. The ICA is sensitive and specific and can achieve on-site rapid detection of swine stool samples. Therefore, the ICA has a great potential for PED diagnosis and prevention.

1. Introduction

Porcine epidemic diarrhea virus (PEDV), a member of the genera Alphacoronavirus in the family Coronaviridae, causes acute diarrhea, vomiting, dehydration and high mortality in seronegative neonatal piglets [1]. Epidemic PEDV strains spread rapidly and have a high mortality, which brings great economic losses to the pig industries [2,3]. As early as the 1970s, PEDV was reported in European and Asian pig industries. Since then, PEDV has spread to the United States, Canada, Mexico, China, South Korea and other countries, and has induced a worldwide disease [4,5]. PEDV has the highest incidence of all the pandemic viruses in China, accounting for about 46% of pandemic viruses [6,7]. Clinically, PEDV and other porcine intestinal coronavirus infections have similar clinical symptoms, causing severe diarrhea, vomiting and atrophic enteritis. However, the other diseases have smaller clinical impacts and are less severe than that caused by PEDV [1,8]. At present, the differential diagnosis of PEDV and other viruses is critical to control viral epidemic diarrhea. It is especially necessary to choose a detection method with high sensitivity, specificity and relatively low cost.

Currently, there are several ways to detect PEDV, such as molecular biological detection methods including nucleic acid probes, polymerase chain reaction (PCR), and loop-mediated isothermal amplification among others. These methods have both high precision and specificity [9–14]. However, they require precise experimental instruments and trained experimenters, and have certain restrictions on promoting grassroots production. Therefore, they are not ideal for on-site rapid detection of PEDV. In addition, immunological detection methods including serum neutralization experiments, immunofluorescence, enzyme-linked immunosorbent assay and immunochromatography

Abbreviations: PEDV, Porcine epidemic diarrhea virus; PRV, Pseudorabies virus; CSFV, Classical swine fever virus; TGEV, Transmissible gastroenteritis virus; PRRSV, Porcine reproductive and respiratory syndrome virus; mAbs, Monoclonal antibodies; Eu, Europium; ICA, Immunochromatographic assay; ROC, Receiver operating characteristic

* Corresponding author. Department of Bioengineering, Guangdong Province Engineering Research Center of Antibody drug and Immunoassay, Jinan University, Guangzhou, 510632, PR China.
** Corresponding author.
*** Corresponding author.
E-mail addresses: 563464890@qq.com (X. Zhang), 59492815@qq.com (A. Jia), tyjaq7926@163.com (Y. Tang).
[1] These three authors contributed equally to this work.

https://doi.org/10.1016/j.talanta.2020.120865
Received 23 October 2019; Received in revised form 22 February 2020; Accepted 24 February 2020
Available online 25 February 2020
0039-9140/

[15–20] have been used to detect PEDV and other pathogens. These detection methods are simple, specific and sensitive. We previously developed a method using the gold nanoparticle signal of a test strip based on monoclonal antibodies prepared with a PEDV isolate [16]. However, its coincidence rate with RT-PCR was only 74.07%. Since the results were not ideal, it is important to establish a more sensitive and accurate immunochromatographic test strip with characters of simple to operate and easy to observe in on-site applications.

Time-resolved fluorescence is fluorescence emitted by rare earth metals. Their chelates have the advantages of unique fluorescence, a narrow emission peak, a high quantum yield, a wide Stokes shift and a long fluorescence lifetime. A long period of fluorescence emission can delay the measurement of a fluorescent signal, allowing it to be distinguished from the background fluorescence that has a shorter half-life [21,22]. Based on these advantages, interference between the excitation light and non-specific fluorescence can be excluded, leading to improvement of both the signal-to-noise ratio and sensitivity [23], making them favourable probes for on-site rapid detection. Commonly used rare earth metals contain europium (Eu) and terbium (Tb) [24]. Europium is widely used throughout bioanalysis [25–30]. Europium nanoparticles (EuNPs) are microspheres prepared by bonding Europium and its chelate to the surface of polystyrene microspheres [31]. Herein, EuNPs are used as a novel material for the preparation of time-resolved fluorescent test strips. The low interference from background fluorescence when using EuNPs results in improved sensitivity compared with conventional fluorescent test strips.

This study developed a optimized immunochromatographic assay (ICA) based on Europium nanoparticles labeled monoclonal antibody (EuNPs-mAb) fluorescent probes. Our work showed that EuNPs-mAb probes are sensitive and specific, have a high coincidence with RT-PCR, and can be used for on-site rapid PEDV detection.

2. Materials and methods

2.1. Reagents and materials

Anti-porcine epidemic diarrhea virus monoclonal antibodies 4A11F11 and 4A11D10 were prepared in our laboratory. Porcine epidemic diarrhea virus (PEDV) strain CHYJ130330, Porcine circovirus (PCV2), Rota virus (RV), Transmissible Gastroenteritis Virus (TGEV) and swine stool samples were obtained from Guangdong Hyde Animal Husbandry and Veterinary Research Institute (Guangdong, China). Pseudorabies virus (PRV) was obtained from Keqian (Wuhan, China), classicalswine fever virus (CSFV) was obtained from Winsun Bio (Guangzhou, China). Nitrocellulose (NC) film (HF18002S25), conjugate pad, sample pad, plastic backing and absorbent pad were purchased from Millipore (Shanghai, China). The goat anti-mouse IgG was purchased from Sanjian (Tianjin, China). Time-resolved fluorescent microspheres, 1-ethyl-3-(3-dimethylaminopropyl) carbodiimide hydrochloride (EDC), N-hydroxysulfosuccinimide (sulfo-NHS) were purchased from ThermoFisher (USA). 4-Morpholineethanesulfonic acid (MES), Hypoxanthine-aminopterin-thymidine (HAT) medium, hypoxanthine-thymidine (HT) medium, Freund's complete adjuvant, Freund's incomplete adjuvant and Tween-20 were purchased from Sigma-Aldrich (USA). D-trehalose, BSA, sucrose, and casein sodium were purchased from Asegene (Guangzhou, China). Sodium hydroxide, $Na_2HPO_4{\cdot}12H_2O$ and $NaH_2PO_4{\cdot}2H_2O$ were purchased from Guangzhou Chemical Reagent Factory (Guangzhou, China). Ultrapure water produced by Milli-Q Ultra Pure System (Millipore, USA) was used throughout the study. All chemicals used were of analytical grade or higher.

2.2. Apparatus

Flashlight (Excitation light: 365 nm, Emitted light; Warsun, China), and the immunofluorescent analyzer were purchased from Lanbo (Guangdong, China). A transmission electron microscope (Philips, Holland) and a particle size analyzer (Malvern, England) were used for the characterization of EuNPs. The following equipments were also used in this study: centrifuge 5810 R (Eppendorf, Germany), XW-80 vortex mixer (Shanghai, China), ultrasonic homogenizer (Ningbo, China), dynabeads MX mixer (Invitrogen, America), programmable strip cutting machine HGS201 (AUTOXUN, China), XYZ3060 platform (Bio-Dot Scientific Equipment, China), electric forced air convection drying oven (TAISITE Instrument, China), magnetic stirrer (Aohua Instrument, China), desktop high speed refrigerated centrifuge (Beckman, America) and pH meter (Mettler Toledo, Switzerland).

2.3. Preparation of Eu nanoparticles labeled mAb (EuNPs-mAb)

The preparation process of EuNPs-4A11F11 was as follows. First, 10 μL of EuNPs were added to 990 μL of 0.1 M MES and mixed. Then, 10 μL of 10 mg/mL EDC and 100 μL of 5 mg/mL sulfo-NHS (diluted with 0.1 M MES) were added, mixed and rotated for 30 min. The mixture was then centrifuged at 15,000 rpm for 20 min, and the precipitate was re-suspended in 1 mL of 0.1 M MES, and 8 μL of 4A11F11 (2 mg/mL) were added. The mixture was rotated for 1 h. Then, 10 μL of 1% BSA were added, mixed and rotated for additional 1 h. After that, the solution was centrifuged at 12,000 rpm for 15 min, and the precipitate was re-suspended in 500 μL of 0.2 M PB (pH 7.4). Finally, an ultrasonic homogenizer was used to disperse the re-suspended solution at 5% power with 5 cycles of 2 s on and 5 s off. A transmission electron microscope (TEM) was used to characterize the EuNPs (Fig. 2a). The hydrodynamic diameter and surface charge of the EuNPs-4A11F11 were measured by dynamic light scattering with a Zettaliter Nano instrument (Fig. 2b and c).

2.4. Optimization of the ICA

The ICA was assembled as regular method (Supplementary material). To optimize the quality of the ICA, the following factors were optimized: 4A11D10 concentration, goat anti-mouse IgG concentration, sample buffer pH, spray volume of EuNPs-mAb, and reaction time. The detailed information can be found in the supplementary material.

2.5. Sensitivity testing of the ICA

To determine the sensitivity of the ICA, concentrated PEDV (virus titer was expressed as $TCID_{50}$, 10^6TCID_{50}/mL; virus concentration was determined using BCA, 80 μg/mL) was diluted into a series of concentrations using negative swine stools as the buffer solution. Then, 100 μL of different sample solutions were sequentially added to the sample holes of the ICA. After 15 min of reacting, the fluorescent images of strips were photographed using a flashlight and the fluorescent intensity was measured by an immunofluorescent analyzer.

2.6. Specificity testing of the ICA

To verify the specificity of the ICA, the ICA was used to detect pseudorabies virus (PRV), porcine circovirus (PCV2), rota virus (RV), classical swine fever virus (CSFV), transmissible gastroenteritis virus (TGEV) and PEDV prepared at the same concentrations using the same procedure described above.

2.7. Stability testing of the ICA

To verify the stability of the ICA, an accelerated aging experiment was used. The detailed information can be found in the supplementary material.

2.8. Detection of PEDV in spiked samples

For the detection of PEDV in spiked samples, concentrated PEDV (virus titer was expressed as $TCID_{50}$, $10^6 TCID_{50}$/mL; virus concentration was determined using BCA, 80 μg/mL) was diluted into a series of concentrations using negative swine stools to make the spiked samples. The final concentrations of PEDV were 1, 2, 4, 8 and 16 μg/mL. Then, 100 μL of the different spiked samples were added to the sample holes of the ICA. The ICA was performed by following the procedure as described above.

2.9. Detection of PEDV in swine stool samples

For detection of PEDV in swine stools, a total of 60 swine stool samples were detected. The fluorescent signal was read by a card reader as described above. The swine stool samples were detected using the ICA and RT-PCR, respectively. The resulting data were analyzed by SPSS 17.0 software.

2.10. Precision experiment of the ICA

To confirm the precision of the ICA, different concentrations of PEDV were tested in intra and inter assay variations. The detailed information is illustrated in the supplementary material.

3. Results and discussion

3.1. The mechanism of the ICA

The ICA contains five parts (Fig. 1 from left to right): a sample pad for filtering liquid samples, a conjugate pad for combining EuNPs-mAb, a NC membrane to allow for the loading of 4A11D10 and goat anti-mouse IgG, an absorption pad for liquid absorption, and a PVC plate for supporting these four components. When the sample solution is added onto the sample pad, it migrates toward the conjugate pad. In the absence of PEDV (negative sample), EuNPs-mAb is not captured by the mAb on the T-line and the fluorescent signal can only be detected on the C-line (Fig. 1). In contrast, if the sample solution contains PEDV, PEDV first binds to the EuNPs-mAb and is captured by the PEDV mAb on the T-line to form a double-antibody sandwich structure, resulting in the appearance of a fluorescent signal on the T-line. Any uncombined EuNPs-mAb is captured by the goat anti-mouse IgG on the C-line and the fluorescent signal can be detected on the C-line.

3.2. Characterization of the EuNPs-4A11F11

After the antibody was coupled with the EuNPs, the size and zeta potential of the EuNPs changed significantly. The EuNPs were characterized by transmission electron microscopy (TEM) (Fig. 2A). The DLS results revealed that the particle size of EuNPs was 312 ± 3.5 nm, and the particle size of EuNPs-4A11F11 was 450 ± 6.3 nm. The changes of the hydrodynamic size showed that the EuNPs increased in size after being coated with the 4A11F11 antibodies (Fig. 2B). When the EuNPs were activated, their surface charge was unchanged, whereas the negative surface charge was significantly reduced after the antibody was coupled (Fig. 2C).

3.3. Parameter optimization of the ICA

To achieve optimal ICA performance, the concentration of capturing antibody and goat anti-mouse IgG, sample buffer pH, spray volume of EuNPs-mAb, and reaction time were optimized. The results showed that 3.5 mg/mL and 4 mg/mL were the optimal concentrations of capturing antibody and goat anti-mouse IgG, respectively, the optimal sample buffer pH was 8.4, the optimal spray volume was 3 μL/cm, and 15 min of reaction time was the optimal condition (Table S1).

First, the concentration of capturing antibody 4A11D10 was optimized, and among the different concentrations (1.5, 2, 2.5, 3, 3.5 and 3.8 mg/mL), 3.5 mg/mL concentration of 4A11D10 showed the best result in positive and negative response, whereas the 3.8 mg/mL concentration caused an obvious decrease of the positive fluorescent intensity and produced unspecific signal in negative sample (Fig. S1). Therefore, 3.5 mg/mL was determined to be the optimal 4A11D10 concentration.

Second, the goat anti-mouse IgG concentration was optimized. Among different concentrations (0.5, 1, 2, 4, and 8 mg/mL), 4 mg/mL

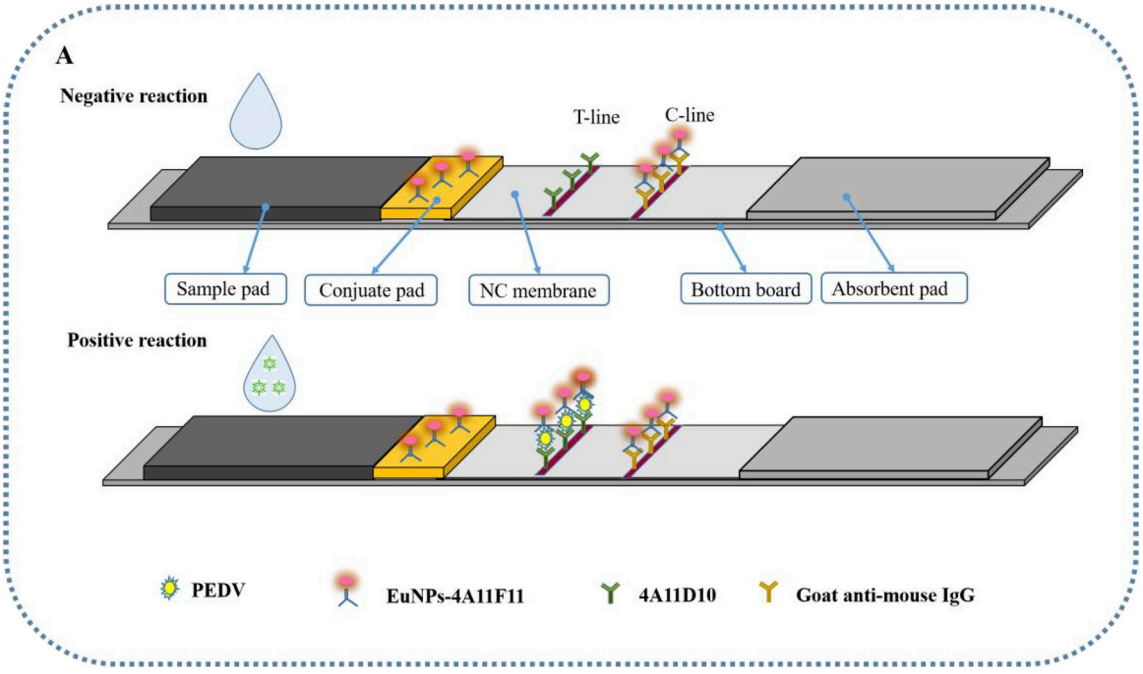

Fig. 1. The simple schematic diagram of the new ICA. Negative reaction. When negative samples were added to the membrane, no fluorescent signal on the T-line was observed; Positive reaction. When positive samples were applied to sample pad, fluorescent signal was visible on the T-line and C-line by a flashlight.

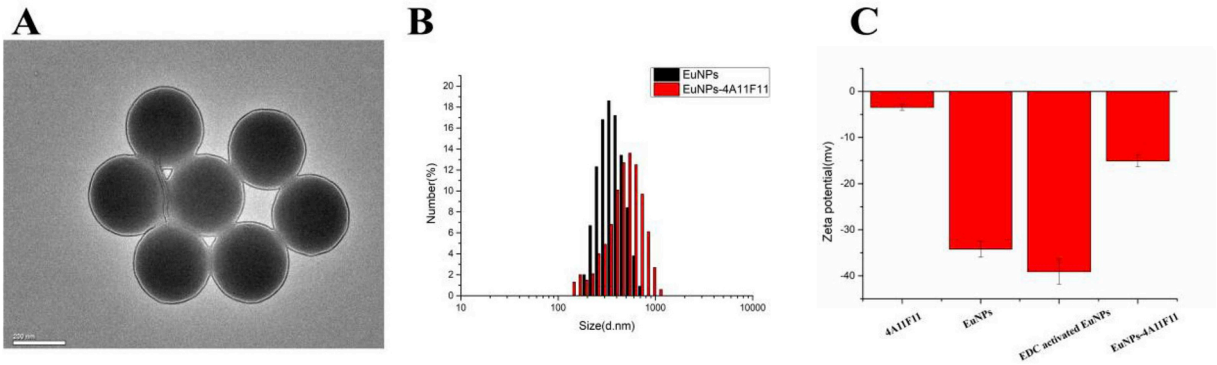

Fig. 2. Characterization of the EuNPs-4A11F11 **A.** TEM images of EuNPs; **B.** Hydrodynamic size of EuNPs and EuNPs-4A11F11; **C.** Surface zeta potential of EuNPs-4A11F11, EuNPs, activated EuNPs and EuNPs-4A11F11.

goat anti-mouse IgG had the highest C-line fluorescent intensity, while the fluorescence intensity was no longer enhanced when the concentration increased to 8 mg/mL, and the signal was not visible when the concentration was too low (Fig. S2). Therefore, 4 mg/mL was determined to be the optimal goat anti-mouse IgG concentration.

Third, the sample buffer pH was optimized by setting to different values (7.4, 8.4, 9.4, 10.4, and 11.4). When the pH of the buffer was 8.4, the best result was obtained, so 8.4 was determined to be the optimal pH (Fig. S3).

Fourth, the spray volume of EuNPs-mAb is known to have a significant effect on the binding ability of the detection antibody, so the spray volume was optimized by setting to different values (1, 2, 3, 4, and 5 μL/cm). When the negative sample was added to the ICA using different spray volumes, 1, 2 and 3 μL/cm had almost the same T-line fluorescent intensity, which were all lower than that of 4 and 5 μL/cm (Fig. S4). When the positive sample was added to the ICA of different spray volumes, 3 μL/cm had the highest T-line fluorescent intensity. Therefore, 3 μL/cm was determined to be the optimal spray volume.

Finally, reaction time is also known to be a significant factor influencing the fluorescence intensity development in the strip test, so the reaction time was optimized by setting to different values (5, 10, 15, and 20 min). When the negative sample was added to the ICA for different reaction times, T-line fluorescent intensity at 20 min was 1.18 times higher than that at 15 min. When the positive sample was added to the ICA, the T-line fluorescent intensity at 20 min was 1.08 times higher than that at 15 min (Fig. S5). Since 1.08 was less than 1.18, the nonspecific reaction increases faster than the specific reaction. Therefore, 15 min was the optimal reaction time.

3.4. Performance of the ICA for PEDV detection

3.4.1. Sensitivity of the ICA

The ICA was designed for efficient PEDV detection. Briefly, the concentrated PEDV (virus titer was expressed as $TCID_{50}$, 10^6TCID_{50}/mL; virus concentration was determined using BCA, 80 μg/mL) was diluted into a series of concentrations (0, 0.03125, 0.0625, 0.125, 0.25, 0.5, 1, 2, 4, 8 and 16 μg/mL) using negative swine stools as diluents. The T-line fluorescent signal increased with increasing PEDV concentration while no T-line fluorescent signal was observed in the negative sample (Fig. 3A). The immunofluorescent analyzer was used to detect the T-line fluorescent intensity to quantify the performance of the ICA (Fig. 3B). The liner detection range was 0.03125–8 μg/mL (3.91×10^2-10^5 $TCID_{50}$/mL) and the coefficient of determination (R^2) was 0.994. The limit of detection (LOD) was estimated to be 0.218 μg/mL (2.725×10^3 $TCID_{50}$/mL) by calculation of LOD = $y_{blank} + 3 \times SD_{blank}$. These results suggest that the ICA can identify PEDV in an accurate and quantitative manner.

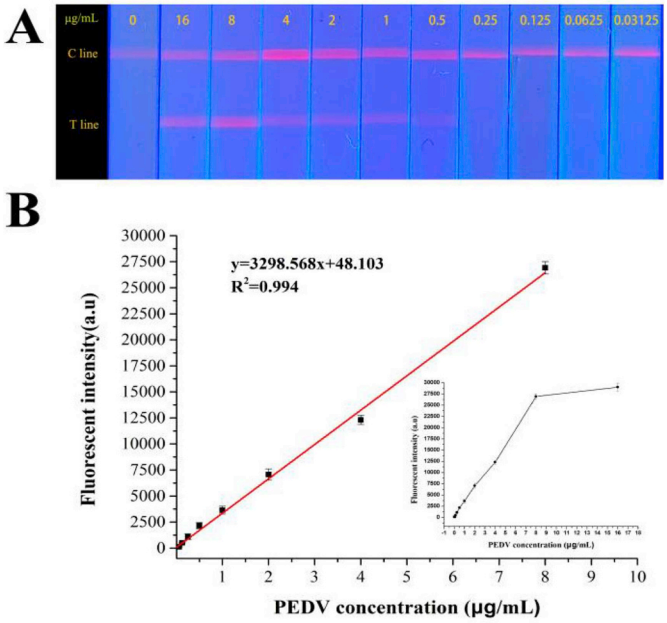

Fig. 3. Sensitivity experiments of the new ICA. **A.** Fluorescent picture of reaction result. As the PEDV concentration increased (from 0.03125 to 16 μg/mL), the fluorescent signal of T-line become more obvious; **B.** A standard curve drawn using the T-line fluorescent intensity detected by the immunofluorescent analyzer.

3.4.2. Specificity of the ICA

To determine the specificity of the ICA, the ICA was used to detect the same concentrations of pseudorabies virus (PRV), porcine circovirus (PCV2), rota virus (RV), classical swine fever virus (CSFV), transmissible gastroenteritis virus (TGEV) and PEDV. The T-line of the PEDV test showed obvious fluorescent signal while the T-line of the other five swine viruses did not show any fluorescent signal (Fig. 4A). These data were further analyzed by gradation histogram based on T-line fluorescent intensity. The results showed that there was approximately 5% cross-reaction with CSFV, and less than 2% cross-reaction with other porcine viruses (Fig. 4B), which further confirmed its acceptable specificity.

3.4.3. Stability of the ICA

The stability of the ICA was confirmed by accelerated aging experiments [32,33] using the same batch of strips. The ICA was performed and the products were stored at 4, 37 and 50 °C for 47 consecutive days and at 25 °C for 148 consecutive days to evaluate the stability. The results showed that the fluorescent intensities of ICA products on T line remained about 85% when stored at 4 °C for 47 days

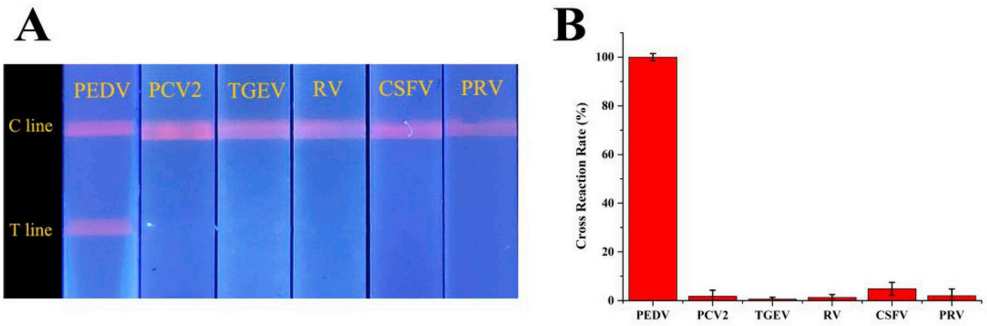

Fig. 4. Specificity of the new ICA. **A.** The fluorescent pictures of different swine viruses were photographed; **B.** Cross-reaction of the new ICA with other swine viruses.

and still remained about 50% after 148 days at room temperature (25 °C) compared to 0 day. The fluorescent intensities after 148 days at 25 °C were still significantly detectable for positive samples qualitative detection (Fig. S6). Theoretically, the ICA products stored at 37 °C for 47 days and at 50 °C for 9 days were equivalent to those stored at room temperature (25 °C) for 178 days and 134 days, respectively (Table S2). In the present study, the ICA exhibited a good stability even after a longer storage time of 148 days at 25 °C according to the room temperature and accelerating test.

3.4.4. Detection of PEDV in spiked samples

In this study, the concentrated PEDV (virus titer was expressed as $TCID_{50}$, $10^6 TCID_{50}$/mL; virus concentration was determined using BCA, 80 μg/mL) was diluted into a series of concentrations using negative swine stools to make spiked samples. The spiked amounts of PEDV were 0.1, 0.2, 0.4, 0.8 and 1.6 μg. As the PEDV concentration increased, the fluorescent signal on the T-line became more intense (Table 1). The relative standard deviation (RSD) was 13.17%, which is below 15%, indicating that the data are credible. The recovery rate of the added PEDV was between 93.54% and 112.5%. Thus, the ICA can be used for detection of PEDV in spiked samples.

3.4.5. Detection of PEDV in swine stool samples

To analyze the performance of the ICA for detection of PEDV in swine stool samples, a total of 60 swine stool samples were analyzed by ICA. After the 15-min reaction, the fluorescent intensity was read by a portable card reader. Based on the fluorescent intensity of ICA, we evaluated the performance with a ROC curve, which can be used to obtain a cut-off value (Fig. 5A). The area under the curve value was 0.8667, indicating that the ICA strip could effectively distinguish the positive and negative samples. The cut-off value was set at a fluorescent intensity of 1920, as calculated by Youden's index [34] from the ROC curve.

In addition, the ICA and RT-PCR results were compared with statistical analysis (Table S5, Fig. 5B). The total coincidence rate of the ICA was 86.67%, indicating that the ICA can be used to accurately analyze swine feces (Table 2).

Table 1
Detection results of PEDV in spiked samples.

Added(μg)	Found(μg)	Recovery(%)	RSD(%)
1.60	1.56 ± 0.13	97.25	8.46
0.80	0.84 ± 0.12	104.88	12.68
0.40	0.45 ± 0.04	112.50	8.68
0.20	0.19 ± 0.01	93.54	1.85
0.10	0.11 ± 0.04	110.00	13.17

Notes: Results were expressed as mean ± S.D.(n = 3).
[a] Recovery(%) = (Found/Added) × 100%.
[b] RSD = (S.D./mean) × 100%.

3.4.6. Precision of the ICA

The precision of the ICA was estimated by the variable coefficient of the detection results of the same batch of ICAs (Table S3) or different batches of ICAs (Table S4). The variable coefficient of all ICAs from the same batch was below 10%, indicating good precision of the same batch ICAs. Furthermore, the variable coefficient of all ICAs from different batches was below 15%, indicating good precision of different batch ICAs. The coefficient of variation of intra and inter assay analysis was within the normal range. Therefore, the ICA has good precision.

4. Conclusions

This study developed a EuNPs-mAb fluorescent probe based immunochromatographic strip for rapid and sensitive detection of porcine epidemic diarrhea virus. The Eu nanoparticles used in the ICA have the advantages of a favourable excitation spectrum bandwidth, a long fluorescence lifetime, a sharp emission peak, a large Stokes displacement, high resolution, and low background. Under optimal conditions, the results of ICA used to detect PEDV indicate that the LOD is 0.218 μg/mL (2.725×10^3 $TCID_{50}$/mL) and the linear detection range is 0.03125–8 μg/mL (3.91×10^2-10^5 $TCID_{50}$/mL). The specificity test results showed that there was approximately 5% cross-reaction between this ICA and CSFV, and the cross-reaction with other porcine viruses was less than 2%. The ICA was also validated for the PEDV detection in swine stool samples with little interference. To compare its accuracy to traditional detection methods, 60 swine stool samples from southern China were investigated with the newly developed ICA and RT-PCR. The Youden's index of the ROC used to find the optimal cut-off value and the positive coincidence rate of these two methods was 91.7%, the negative coincidence rate was 79.2%, and the total coincidence rate was 86.67%. In conclusion, the ICA is sensitive and specific and can be applied to on-site rapid detection of swine stool samples. Therefore, the ICA has great potential for PEDV diagnosis and prevention.

CRediT authorship contribution statement

Fei Xu: Conceptualization, Methodology. **Zhiyuan Jin:** Writing - original draft, Data curation. **Siyi Zou:** Formal analysis, Investigation. **Chaoqun Chen:** Software. **Qifang Song:** Validation, Resources. **Shengchao Deng:** Resources, Investigation. **Wei Xiao:** Validation, Software. **Xiaoli Zhang:** Supervision. **Aiqing Jia:** Resources, Supervision. **Yong Tang:** Conceptualization, Project administration.

Declaration of competing interest

The authors declare that they have no known competing financial interests or personal relationships that could have appeared to influence the work reported in this paper.

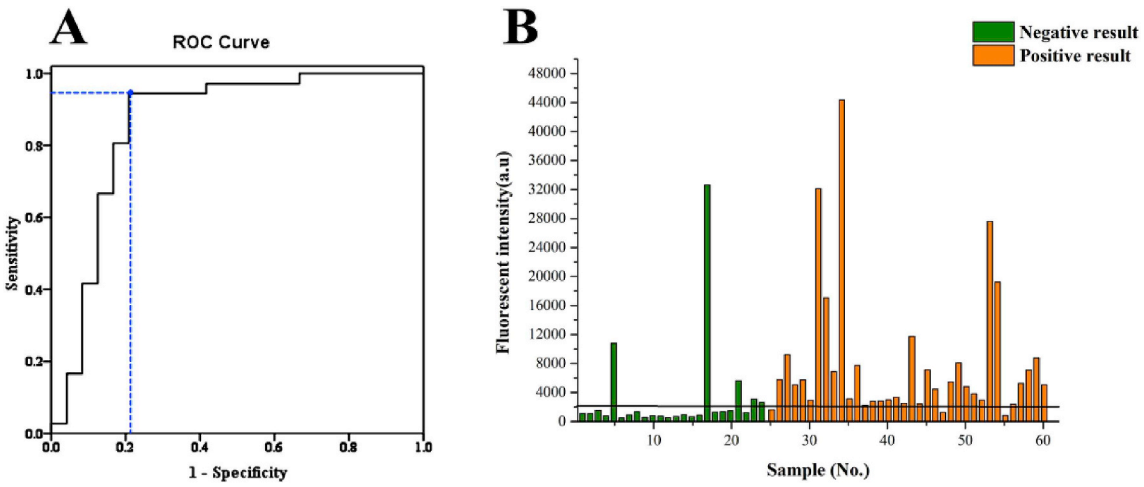

Fig. 5. A. Receiver operating characteristic (ROC) analysis of swine stool samples based on parameter of ICA for detecting PEDV; **B.** The fluorescent intensity result of 60 swine stool samples tested by ICA, the negative and positive result validated by RT-PCR.

Table 2
The total coincidence rate of RT-PCR and the ICAs detection.

Group	Result	RT-PCR		Total
		Positive	Negative	
ICA	Positive	33	5	38
	Negative	3	19	22
Total		36	24	60

[a] Positive coincidence rate: 91.7%.
[b] Negative coincidence rate: 79.2%.
[c] Test coincidence rate: 86.67%.

Acknowledgment

This work was supported by National Key Research and Development Program of China (2016YFD0500600). We thanked Guangdong Haid Institute of animal Husbandry & Veterinary for providing pig fecal samples.

Appendix A. Supplementary data

Supplementary data to this article can be found online at https://doi.org/10.1016/j.talanta.2020.120865.

References

[1] K. Jung, L.J. Saif, Porcine epidemic diarrhea virus infection: etiology, epidemiology, pathogenesis and immunoprophylaxis, Vet. J. 204 (2) (2015) 134–143.
[2] C.-M. Lin, L.J. Saif, D. Marthaler, Q. Wang, Evolution, antigenicity and pathogenicity of global porcine epidemic diarrhea virus strains, Virus Res. 226 (2016) 20–39.
[3] D. Song, B. Park, Porcine epidemic diarrhoea virus: a comprehensive review of molecular epidemiology, diagnosis, and vaccines, Virus Gene. 44 (2) (2012) 167–175.
[4] E. Wood, An apparently new syndrome of porcine epidemic diarrhoea, Vet. Rec. 100 (12) (1977) 243.
[5] N. Van Diep, M. Sueyoshi, J. Norimine, T. Hirai, O. Myint, A.P.P. Teh, U.Z. Izzati, N. Fuke, R. Yamaguchi, Molecular characterization of US-like and Asian non-S INDEL strains of porcine epidemic diarrhea virus (PEDV) that circulated in Japan during 2013–2016 and PEDVs collected from recurrent outbreaks, BMC Vet. Res. 14 (1) (2018) 96.
[6] F. Zheng, J. Huo, J. Zhao, H. Chang, X. Wang, L. Chen, C. Wang, Molecular characterization and phylogenetic analysis of porcine epidemic diarrhea virus field strains in Central China during 2010-2012 outbreaks, Bing du xue bao = Chinese journal of virology 29 (2) (2013) 197–205.
[7] D. Wang, L. Fang, S. Xiao, Porcine epidemic diarrhea in China, Virus Res. 226 (2016) 7–13.
[8] C. Lee, Porcine epidemic diarrhea virus: an emerging and re-emerging epizootic swine virus, Virol. J. 12 (1) (2015) 193.
[9] D. Diel, S. Lawson, F. Okda, A. Singrey, T. Clement, M. Fernandes, J. Christopher-Hennings, E. Nelson, Porcine epidemic diarrhea virus: an overview of current virological and serological diagnostic methods, Virus Res. 226 (2016) 60–70.
[10] Q. Zhang, X. Liu, Y. Fang, P. Zhou, Y. Wang, Y. Zhang, Detection and phylogenetic analyses of spike genes in porcine epidemic diarrhea virus strains circulating in China in 2016–2017, Virol. J. 14 (1) (2017) 194.
[11] Y. Su, Y. Liu, Y. Chen, G. Xing, H. Hao, Q. Wei, Y. Liang, W. Xie, D. Li, H. Huang, A novel duplex TaqMan probe-based real-time RT-qPCR for detecting and differentiating classical and variant porcine epidemic diarrhea viruses, Mol. Cell. Probes 37 (2018) 6–11.
[12] J. Liu, L.-m. Li, J.-q. Han, T.-r. Sun, X. Zhao, R.-t. Xu, Q.-y. Song, A TaqMan probe-based real-time PCR to differentiate porcine epidemic diarrhea virus virulent strains from attenuated vaccine strains, Mol. Cell. Probes 45 (2019) 37–42.
[13] W. Yuan, Y. Li, P. Li, Q. Song, L. Li, J. Sun, Development of a nanoparticle-assisted PCR assay for detection of porcine epidemic diarrhea virus, J. Virol. Methods 220 (2015) 18–20.
[14] F.-X. Wang, D.-Y. Yuan, Y.-N. Jin, L. Hu, Z.-Y. Sun, Q. He, S.-H. Zhao, S.-B. Zhan, Y.-J. Wen, Reverse transcription cross-priming amplification–nucleic acid test strip for rapid detection of porcine epidemic diarrhea virus, Sci Rep-Uk 6 (2016) 24702.
[15] H. Lin, H. Zhou, L. Gao, B. Li, K. He, H. Fan, Development and application of an indirect ELISA for the detection of antibodies to porcine epidemic diarrhea virus based on a recombinant spike protein, BMC Vet. Res. 14 (1) (2018) 243.
[16] H. Bian, F. Xu, Y. Jia, L. Wang, S. Deng, A. Jia, Y. Tang, A new immunochromatographic assay for on-site detection of porcine epidemic diarrhea virus based on monoclonal antibodies prepared by using cell surface fluorescence immunosorbent assay, BMC Vet. Res. 15 (1) (2019) 32.
[17] F. Okda, X. Liu, A. Singrey, T. Clement, J. Nelson, J. Christopher-Hennings, E.A. Nelson, S. Lawson, Development of an indirect ELISA, blocking ELISA, fluorescent microsphere immunoassay and fluorescent focus neutralization assay for serologic evaluation of exposure to North American strains of Porcine Epidemic Diarrhea Virus, BMC Vet. Res. 11 (1) (2015) 180.
[18] Z. Wang, Y. Jiyuan, C. Su, Q. Xinyuan, T. Lijie, L. Yijing, Development of an antigen capture enzyme-linked immunosorbent assay for virus detection based on porcine epidemic diarrhea virus monoclonal antibodies, Viral Immunol. 28 (3) (2015) 184–189.
[19] K.-S. Lyoo, M. Yeom, J. Kim, D. Kim, G. Ha, W. Na, V.P. Le, D. Song, Development of rapid immunochromatographic strip test for the detection of porcine epidemic diarrhoea virus, Vet. Rec. 181 (22) (2017) 596.
[20] H. Shen, H. Chen, Z. Cheng, L. Ma, L. Huang, M. Xiao, W. Xiao, K. Xie, Y. Tang, A novel fluorescent immunochromatographic strip combined with pocket fluorescence observation instrument for rapid detection of PRV, Anal. Bioanal. Chem. 410 (29) (2018) 7655–7661.
[21] B.R. Masters, Molecular fluorescence: principles and applications, J. Biomed. Optic. 18 (3) (2013) 039901.
[22] D.J. Birch, R.E. Imhof, Time-domain fluorescence spectroscopy using time-correlated single-photon counting, Topics in fluorescence spectroscopy (2002) 1–95 Springer.
[23] U. Cho, D.P. Riordan, P. Ciepla, K.S. Kocherlakota, J.K. Chen, P.B. Harbury, Ultrasensitive optical imaging with lanthanide lumiphores, Nat. Chem. Biol. 14 (1) (2018) 15.
[24] Y. Pan, X. Xie, Q. Huang, C. Gao, Y. Wang, L. Wang, B. Yang, H. Su, L. Huang, W. Huang, Inherently Eu2+/Eu3+ codoped Sc2O3 nanoparticles as high--performance nanothermometers, Adv. Mater. 30 (14) (2018) 1705256.
[25] G. Muller, Luminescent chiral lanthanide (III) complexes as potential molecular probes, Dalton Trans. 44 (2009) 9692–9707.
[26] J. Liu, J. Zhao, P. Petrochenko, J. Zheng, I. Hewlett, Sensitive detection of influenza viruses with Europium nanoparticles on an epoxy silica sol-gel functionalized polycarbonate-polydimethylsiloxane hybrid microchip, Biosens. Bioelectron. 86 (2016) 150–155.

[27] E. Juntunen, T. Myyryläinen, T. Salminen, T. Soukka, K. Pettersson, Performance of fluorescent europium (III) nanoparticles and colloidal gold reporters in lateral flow bioaffinity assay, Anal. Biochem. 428 (1) (2012) 31–38.
[28] T. Salminen, E. Juntunen, S.M. Talha, K. Pettersson, High-sensitivity lateral flow immunoassay with a fluorescent lanthanide nanoparticle label, J. Immunol. Methods 465 (2019) 39–44.
[29] R.-L. Liang, X.-P. Xu, T.-C. Liu, J.-W. Zhou, X.-G. Wang, Z.-Q. Ren, F. Hao, Y.-S. Wu, Rapid and sensitive lateral flow immunoassay method for determining alpha feto-protein in serum using europium (III) chelate microparticles-based lateral flow test strips, Anal. Chim. Acta 891 (2015) 277–283.
[30] S.-J. Yeo, D.T. Bao, G.-E. Seo, C.T. Bui, N.T.V. Anh, T.T.T. Tien, N.T.P. Linh, H.-J. Sohn, C.-K. Chong, H.-J. Shin, Improvement of a rapid diagnostic application of monoclonal antibodies against avian influenza H7 subtype virus using Europium nanoparticles, Sci Rep-Uk 7 (1) (2017) 7933.
[31] K.-Y. Xing, J. Peng, D.-F. Liu, L.-M. Hu, C. Wang, G.-Q. Li, G.-G. Zhang, Z. Huang, S. Cheng, F.-F. Zhu, Novel immunochromatographic assay based on Eu (III)-doped polystyrene nanoparticle-linker-monoclonal antibody for sensitive detection of Escherichia coli O157: H7, Anal. Chim. Acta 998 (2018) 52–59.
[32] O.U. Press, New CLSI Guideline for Evaluation of Stability of In Vitro Diagnostic Reagents 41 (1) (2010) 18–19.
[33] S.K. Vashist, J.H. Luong, Handbook of Immunoassay Technologies: Approaches, Performances, and Applications, Academic Press2018.
[34] K. Hajian-Tilaki, Receiver operating characteristic (ROC) curve analysis for medical diagnostic test evaluation, Caspian journal of internal medicine 4 (2) (2013) 627.